Aircraft Observations for Improved Physical Parameterization for Seasonal Prediction

Djamal Khelif
Department of Mechanical and Aerospace Engineering
University of California, Irvine
Irvine, CA 92697-3975
phone: (949) 824-7437 fax: (949) 824-8585 email: dkhelif@uci.edu

Award Number: N00014-12-1-0444

LONG-TERM GOALS

The long-terms goals of our research are to understand and parameterize the physics of air-sea interaction and the Marine Atmospheric Boundary Layer (MABL) over a wide spectrum of wind speeds, sea state and cloud coverage.

OBJECTIVES

The objective of this effort is to obtain extensive measurements in the MABL under different cloud fractions specially aimed at quantifying various statistical quantities needed to examine and develop PDF-based cloud and turbulence parameterizations. The data set produced will help us understand the characteristics of empirical PDF of various dynamic and thermodynamic variables and their relevant turbulent statistics. In particular, we seek to understand the interplay among various physical processes in the cloudy boundary layer including surface forcing, longwave radiative cooling and shortwave radiative warming, turbulence transport, cloud microphysics, and entrainment and relate these processes to the PDF analyses. These measurements and analyses will be used by our collaborating modelers to evaluate different PDF cloud parameterization schemes in meso- and large scale forecast models with the goal of developing new parameterizations.

APPROACH

To achieve these objectives, we participated in the Unified Physical Parameterization for Extended Forecast (UPPEF) experiment and conducted aircraft measurements in the MABL off Monterey Bay under various cloud fraction conditions in the summer of 2012. We used the CIRPAS Twin Otter (TO) research aircraft that we instrumented with proven turbulence instrumentation for previous ONR projects to measure mean and turbulent wind components, temperature and humidity and associated air-sea fluxes. Specifically for this study, we made improvements to the instruments especially for humidity with the use of the fast-response UCI-modified LI-7200 enclosed path and the LI-7500 and the open-path H2O/CO2 analyzers in addition to our modified fast-response Krypton hygrometer. The radome wind gust sensing system was also completely overhauled. The main instrumentation on the TO is shown in Fig. 1. Similar measurements were also made with the Controlled Towed Vehicle (CTV). This is a modified target drone that we have been developing for air-sea interaction measurements and equipped with instruments to that of the TO. The CTV is towed by the TO via a thin

Report Documentation Page

Form Approved
OMB No. 0704-0188

1. REPORT DATE	2. REPORT TYPE	3. DATES COVERED
30 SEP 2013		**00-00-2013 to 00-00-2013**

4. TITLE AND SUBTITLE	5a. CONTRACT NUMBER
Aircraft Observations for Improved Physical Parameterization for Seasonal Prediction	5b. GRANT NUMBER
	5c. PROGRAM ELEMENT NUMBER
6. AUTHOR(S)	5d. PROJECT NUMBER
	5e. TASK NUMBER
	5f. WORK UNIT NUMBER
7. PERFORMING ORGANIZATION NAME(S) AND ADDRESS(ES) **University of California, Irvine,Department of Mechanical and Aerospace Engineering,Irvine,CA,92697-3975**	8. PERFORMING ORGANIZATION REPORT NUMBER
9. SPONSORING/MONITORING AGENCY NAME(S) AND ADDRESS(ES)	10. SPONSOR/MONITOR'S ACRONYM(S)
	11. SPONSOR/MONITOR'S REPORT NUMBER(S)

12. DISTRIBUTION/AVAILABILITY STATEMENT
Approved for public release; distribution unlimited

13. SUPPLEMENTARY NOTES

14. ABSTRACT

15. SUBJECT TERMS

16. SECURITY CLASSIFICATION OF:			17. LIMITATION OF ABSTRACT	18. NUMBER OF PAGES	19a. NAME OF RESPONSIBLE PERSON
a. REPORT **unclassified**	b. ABSTRACT **unclassified**	c. THIS PAGE **unclassified**	**Same as Report (SAR)**	**14**	

steel cable and is capable of active height-keeping as low as 10 m above sea level and 300 m below the TO.

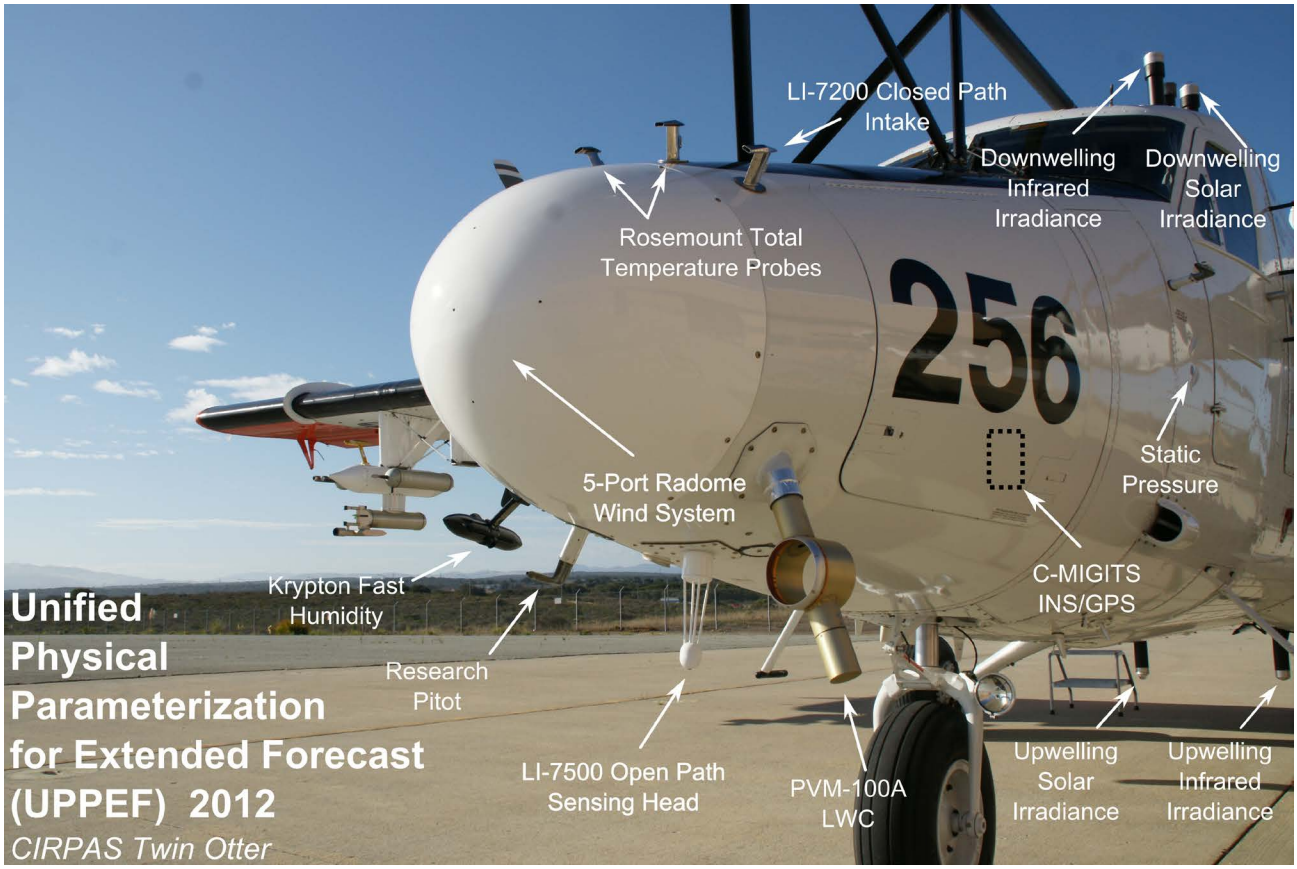

Figure 1. Turbulence and meteorological instrumentation installed on the CIRPAS Twin Otter aircraft for UPPEF 2012.

The TO flew a total of 12 UPPEF flights (and one overland wind lidar flight) depending on the cloud cover condition and the objectives of each given flight several track patterns varying from "L", "U", "S", box, and long linear outbound/inbound transects were flown as shown in Fig. 2. The 3-D flight track with contours of potential temperature, θ, and dewpoint temperature Td for the long linear outbound/inbound transects pattern on September 26, 2013 are also shown in Fig. 2. It shows that boundary layer height (identified with abrupt change θ and in Td at the inversion) steadily increased with offshore distance.

WORK COMPLETED

High quality turbulence and meteorological measurements were obtained from the 12 UPPEF flights. The data were processed immediately after completion of each flight for quick-look and analysis. More rigorous processing and data quality control was systematically performed on data from all instruments we contributed and on data from instruments from other PIs (like the radiation package) that are

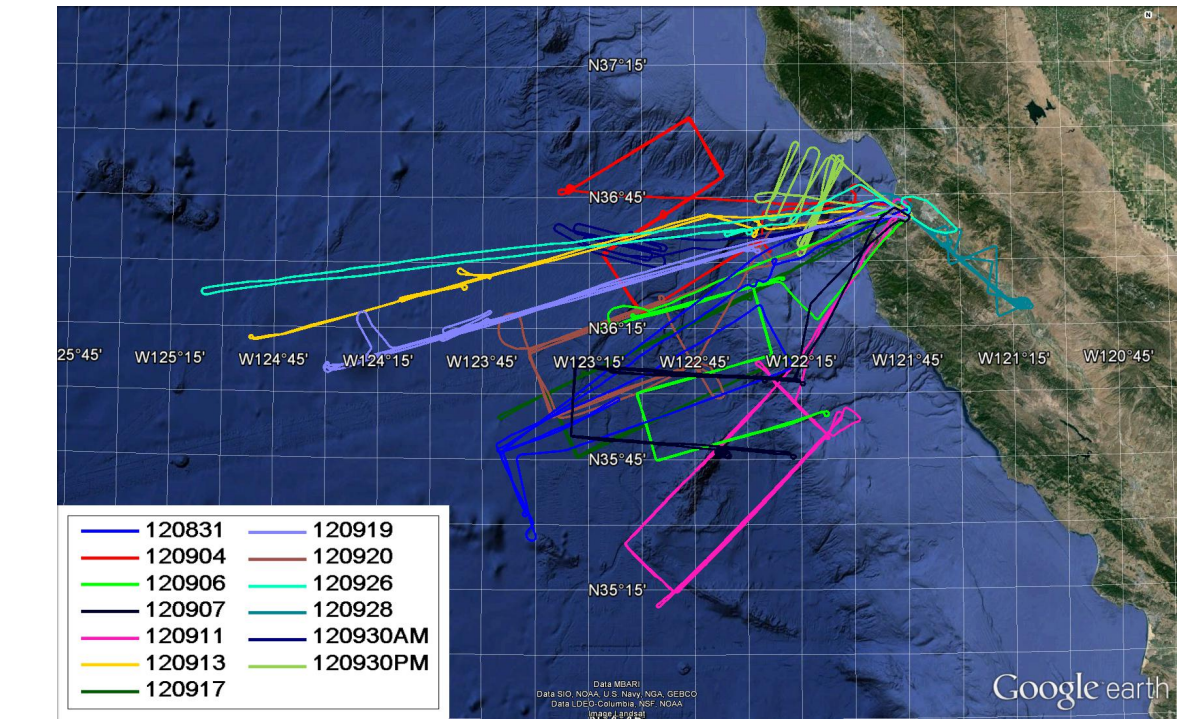

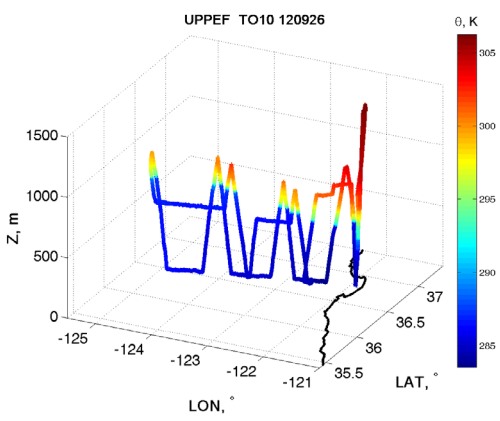

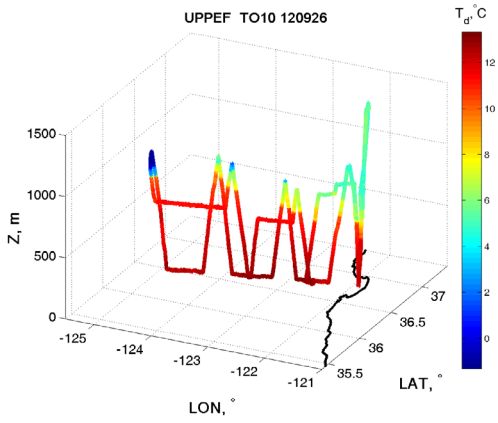

Figure 2. Twin Otter 2-D flight tracks during UPPEF where each flight is identified by its YYMMDD UTC date in the legend (top); 3-D track on the long outbound transect and back on September 26, 2012 with contours of potential temperature, θ, (bottom, left) and dewpoint temperature T_d (bottom, right). Note the increase in boundary layer height (identified with abrupt change θ and in T_d at the inversion) with offshore distance.

required for our research effort. Overall, the instruments performed very well as summarized in Table 1. There were two main data system on the aircraft: CIRPAS's and UCI's. Data from the TO instruments listed in this table were either recorded on the UCI data system (blue background) or CIRPAS's (yellow background) or on both (purple background) for redundancy. There was also a redundancy in many of the sensing systems to ensure that no data are lost due to instrument malfunction. A good example of this is the humidity that was measured by 3 UCI's fast-response instruments and CIRPAS's reference chilled mirror slow-response dewpointer. Water vapor density

(absolute humidity) data from these 4 sensors are shown in Fig. 3 for September 07, 2013 flight. The UCI modified krypton KH2O and the open path LI-7500 ranges were deliberately set for higher humidity values typical of those encountered near the ocean surface which explains why their signals are "clipped" at lower humidity values. The detailed plot of the up and down soundings through the inversion on the lower panel of Fig. 3 illustrates the lag in the chilled mirror response as well as an artificial oscillation on its signal due the Peltier thermoelectric mirror cooling having a hard time adjusting to fast transition from very dry to moist air during the descent soundings.

Table 1. Aircraft instrumentation performance summary during UPPEF experiment in 2012. Data from instruments with blue and light purple background are logged on UCI data system. Note that TO11 (09/28/2012) was an overland flight dedicated to Dave Emmitt's wind lidar.

Unified Physical Parameterization for Extended Forecast (UPPEF) Aug-Sep 2012

Contact Scientist		UTC Day	08/31	09/04	09/06	09/07	09/11	09/13	09/17	09/19	09/20	09/26	09/28	09/30	09/30
		Instrument / Parameter	TO1	TO2	TO3	TO4	TO5	TO6	TO7	TO8	TO9	TO10	TO11 xx	TO12	TO13
dkhelif@uci.edu	Temp	Rosemount Temperature (UCI)													
hjonsson@nps.edu		Rosemount Temperature (CIRPAS)													
dkhelif@uci.edu	Humidity	Fast LI-COR 7200 Humidity (UCI)													
dkhelif@uci.edu		Fast LI-COR 7500 Humidity (UCI)													
dkhelif@uci.edu		Fast Mod. Krypton Hygrometer (UCI)												xxx	xxx
hjonsson@nps.edu		Edge-Tech Vigilent Dewpoint (CIRPAS)													
dkhelif@uci.edu	CO2	Fast LI-COR 7500 CO2 (UCI)													
dkhelif@uci.edu		Fast LI-COR 7200 CO2 (UCI)													
dkhelif@uci.edu	Alt	Roke MRA II Radar Altimeter (UCI)													
hjonsson@nps.edu		Radar Altimeter (CIRPAS)													
hjonsson@nps.edu	Winds	Static Pressure (CIRPAS)													
dkhelif@uci.edu		Radome Gust System (UCI) (x)													
dkhelif@uci.edu	INS / GPS	C-MIGITS (UCI)													
dkhelif@uci.edu		OXTS RT3003 (UCI)													
dkhelif@uci.edu		OXTS Base Station (UCI)													
hjonsson@nps.edu		C-MIGITS (CIRPAS)													
hjonsson@nps.edu		Novatel (CIRPAS)													
hjonsson@nps.edu		TansVector(CIRPAS)													
hjonsson@nps.edu	Radiation	IR SST KT19 (CIRPAS)													
dkhelif@uci.edu		Upward-looking IR Temperature KT19 (UCI)													
bucholtz@nrlmry.navy.mil		Upwelling SW Radiometer (NRL / CIRPAS)													
bucholtz@nrlmry.navy.mil		Upwelling LW Radiometer (NRL / CIRPAS)													
bucholtz@nrlmry.navy.mil		Downwelling SW Radiometer (NRL / CIRPAS)													
bucholtz@nrlmry.navy.mil		Downwelling LW Radiometer (NRL / CIRPAS)													
hjonsson@nps.edu	Clouds / Aerosols	TSI 3025 UFCPC (CIRPAS)													
hjonsson@nps.edu		PCASP (CIRPAS)													
hjonsson@nps.edu		FSSP-100 (CIRPAS)													
hjonsson@nps.edu		CAPS (CIRPAS)													
hjonsson@nps.edu		PVM-100A LWC													
rkwoods@nps.edu		DMT-CCN (CIRPAS)													
dkhelif@uci.edu		Controlled Towed Vehicle (CTV) (UCI)													
gde@swa.com		TODWL (Simpson Weather Associates)													

Data System	UCI	CIRPAS and UCI	CIRPAS	SWA	
Instruments Status	Operational	Oscillations	Some Data	No data	Removed	QC Needed
Footnotes	(x) Different processing		(xx) Over Land		(xxx) Clipped

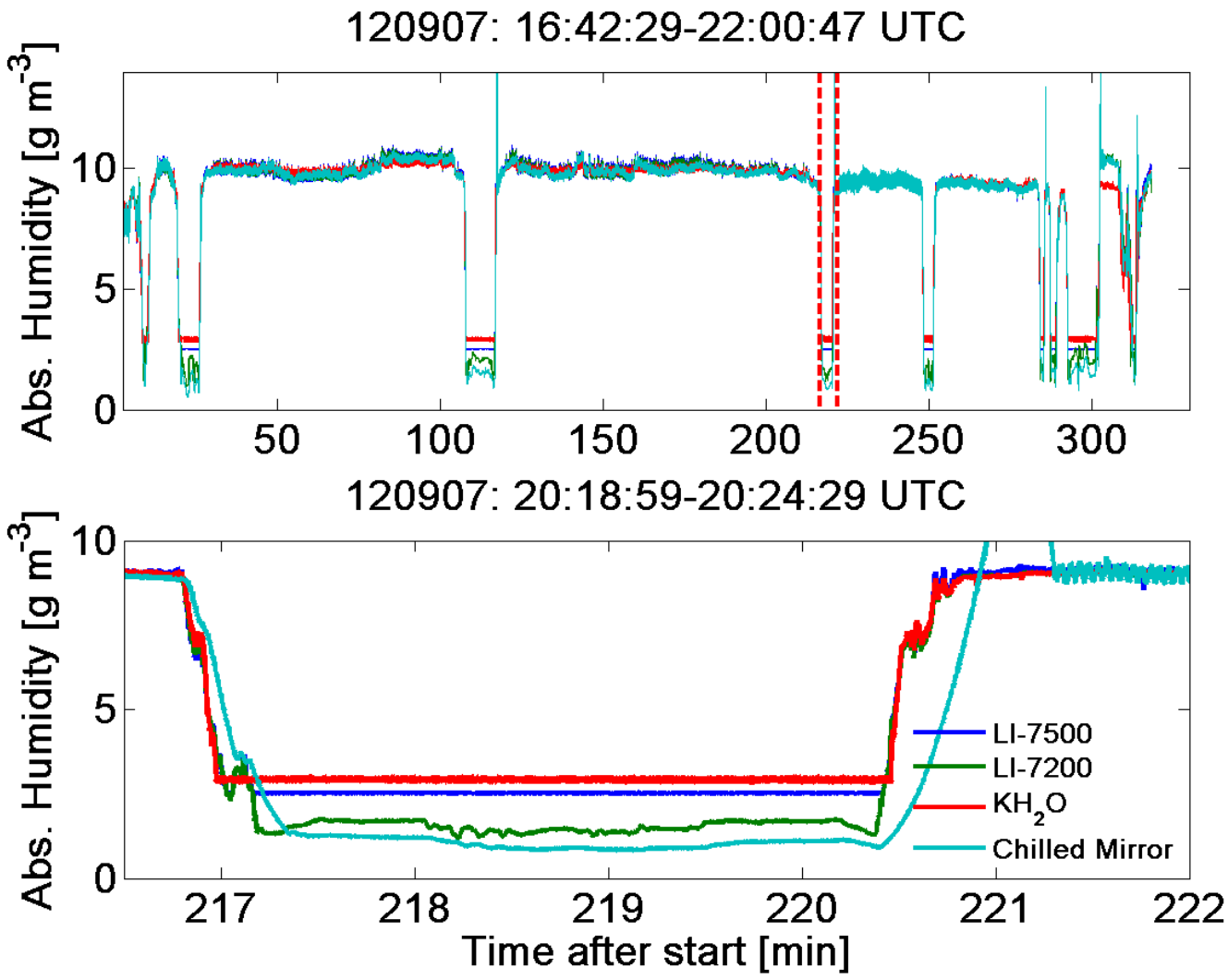

Figure 3. Absolute humidity from UCI fast-response sensors LI-7500 (blue), LI-7200 (green), krypton KH2O (red) and CIRPAS slow-response chilled mirror (cyan). Data are from most of September 07, 2012 flight (top panel) and from the section delineated by red dotted vertical lines (bottom panel).

So far 2 processing iterations were performed on data from all flights. The UCI 40-Hz data set and its descriptive "header" file are available on our data server at this URL:
http://wave.eng.uci.edu/files/UPPEF/datacuts/TO/

RESULTS

Preliminary analysis of the data was performed and we present in this section sample results from the TO measurements and then results from the CTV and discussion of the significant improvements we made to this platform in the past year. Data from each TO flight were first separated into soundings legs and straight and level runs. Eddy correlation fluxes and mean variables were calculated from 3-minutes (corresponding to ~10 km) contiguous segments that were "cut" on all level and straight runs. The ogive method was used to determine the flux estimates as the asymptote value towards the low-frequencies on the cumulative integral (integration done from high to low frequencies) of the cross-

spectrum between the wind vertical component and the relevant variable. Results from 211 lowest levels (~45 m or less) segments are shown on Fig. 4 (means) and Fig. 5 (fluxes) for all UPPEF flights except for the September 28, 2012 flight which was dedicated for the Simpson Associates wind lidar measurements overland. Each green dot on these plots represents data from one 10-km segment and the blue line represents the averages from all segments on the given flight. In general, the variability and trend of the fluxes reflect those of the means of the variables they are associated with.

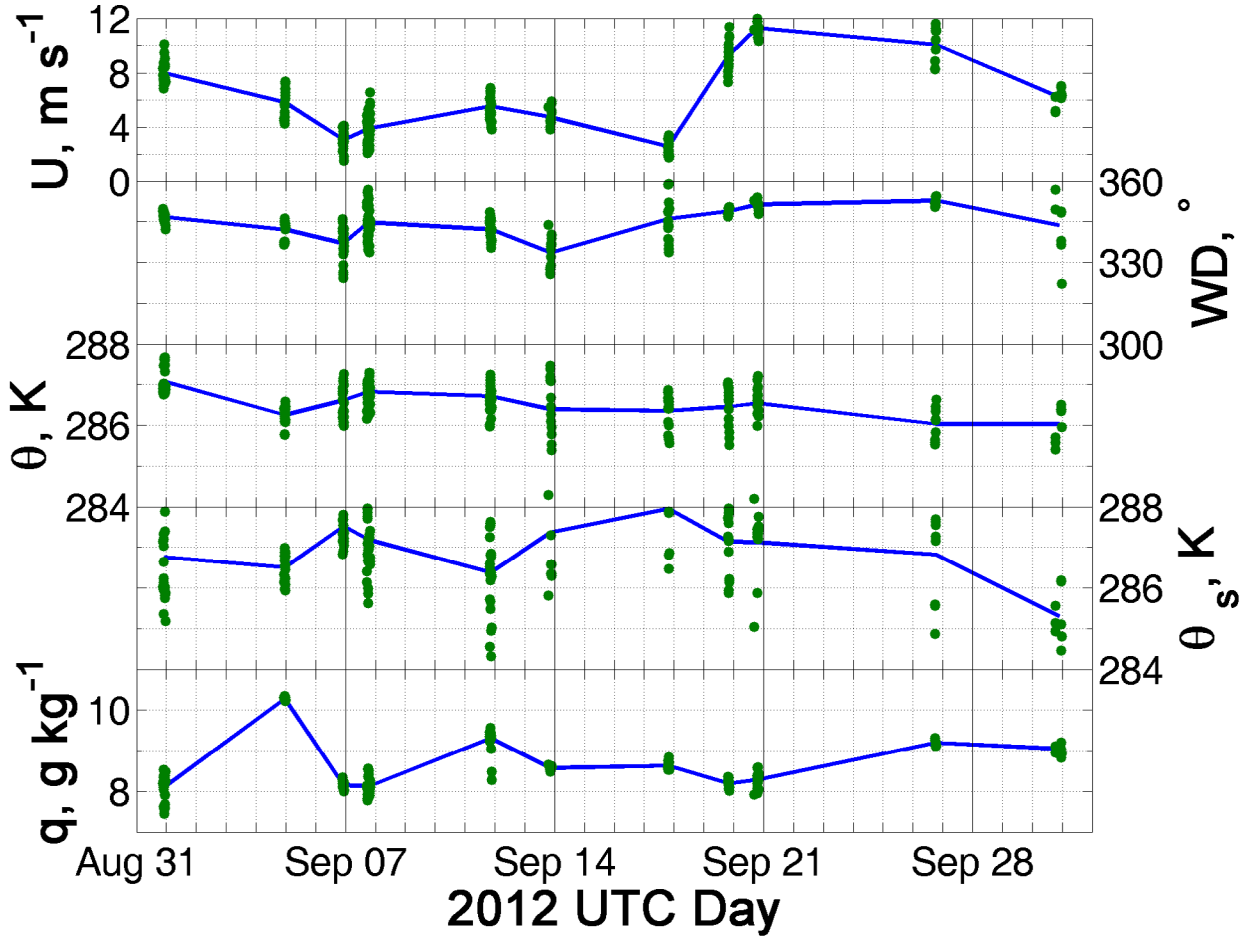

Figure 4. Mean variables obtained from 211 3-minute (~ 10 km) segments from straight and level runs at $z \leq 45$ m. Each green dot represents the average from one such segment and the blue line the flight average of (from to bottom) wind speed, wind direction, air potential temperature, radiometric sea surface temperature and specific humidity.

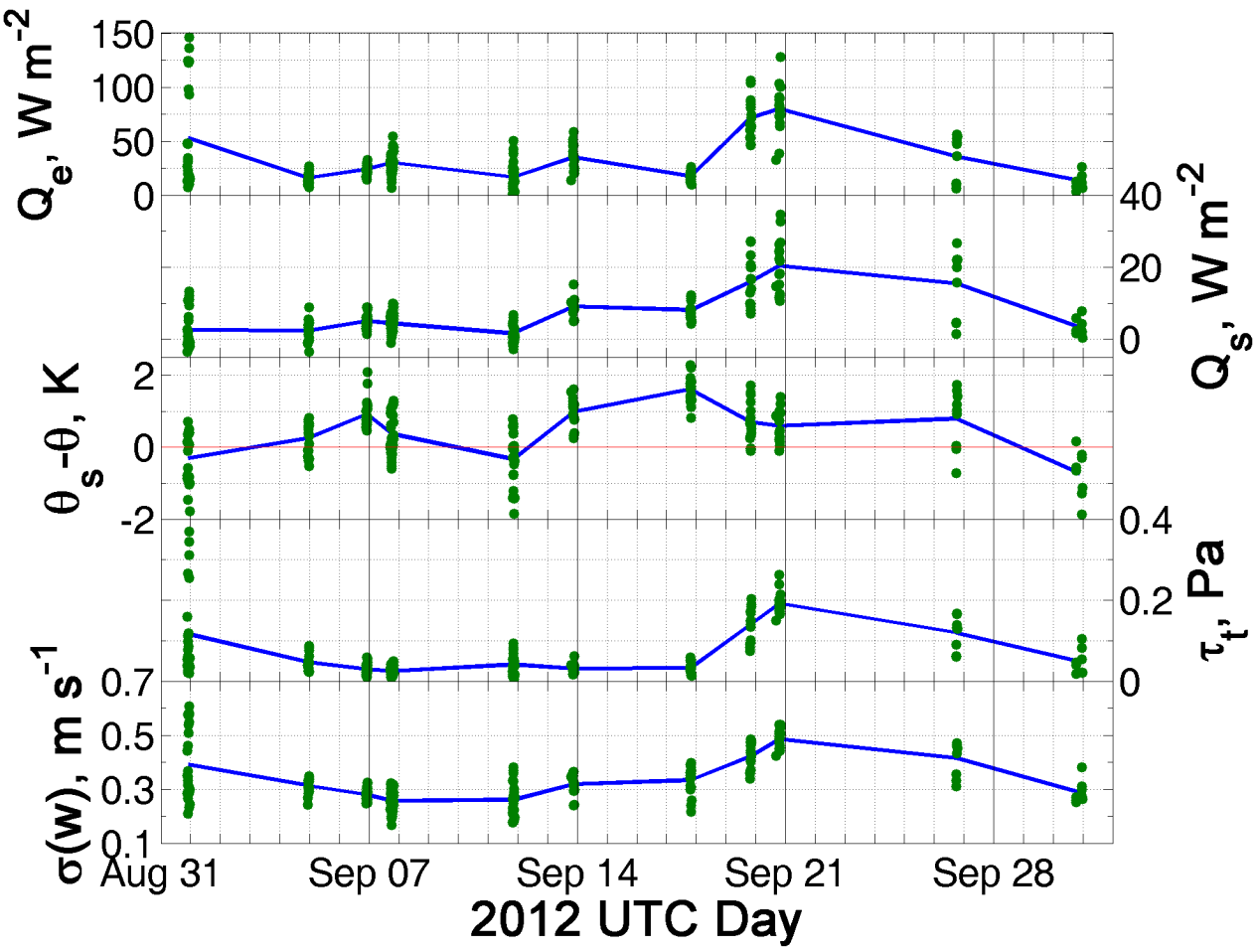

Figure 5. Eddy correlation fluxes obtained from 211 3-minute (~ 10 km) segments from straight and level runs at $z \leq 45$ m. Each green dot represents the estimate from one such segment and the blue line the flight average of (from to bottom) , latent heat flux, sensible heat flux, sea surface-air potential temperatures difference, stress and standard deviation of the wind vertical component.

While expected natural variability due spatial inhomogeneities of the mean quantities and fluxes within each flight is observed on most flights, the variability of the fluxes on the first UPPEF flight (August 31, 2013) stands out. This is due to a very strong (3 ºC) SST front that was present on that day (Fig. 6). The originally planned "L" flight pattern had to be altered on-the-fly after the SST front was detected and straight and levels runs at 33 m and at 95 m across the SST front were flown. From these runs, time series of turbulent fluxes were calculated using the running averaging technique with a 180-s (~10 km) sliding window. Results showing the air-sea interaction response to the SST front are shown in Fig. 7. A dramatic enhancement of turbulence intensity and turbulent fluxes is observed on the high temperature side of the SST front. On the 33-m TO run, the sensible heat flux increased from ~0 to ~14 W m^{-2}, the latent heat flux increased from 10 to ~160 W m^{-2} and the total stress increased from ~0.02 to 0.40 Pa. The standard deviations of the vertical wind speed, horizontal wind speed and water vapor density jumped from 0.24 to 0.60 m s^{-1}, 0.43 to 1.00 m s^{-1} and 0.10 to 0.27 g m^{-3}, respectively, when moving from the cool side to the warm side of the SST front. The very large increase in latent heat flux is due to dryer air over the warm SST side and the presence of structures of different scales in the humidity signal. Similar observation can be made for the data from the 95-m run.

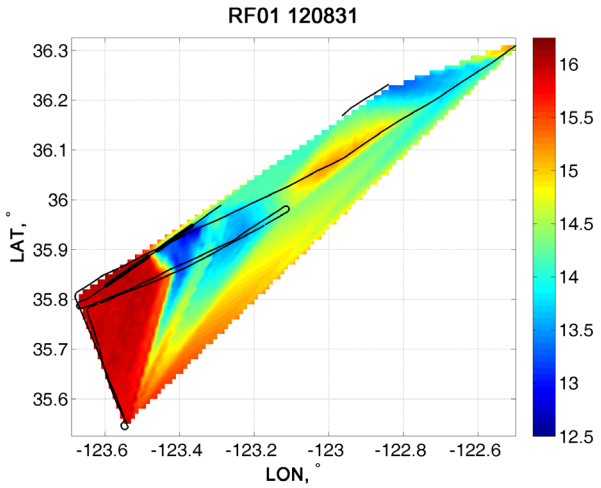

Figure 6. SST contour obtained from the Twin Otter IR pyrometer measurements on August 31, 2012 flight. The track of the aircraft legs at ~33 m and ~95 m are shown with a thin black line. The two thicker black lines are the two segments of the 33-m leg from which statistics on cool and warm sides of the SST front are given the text.

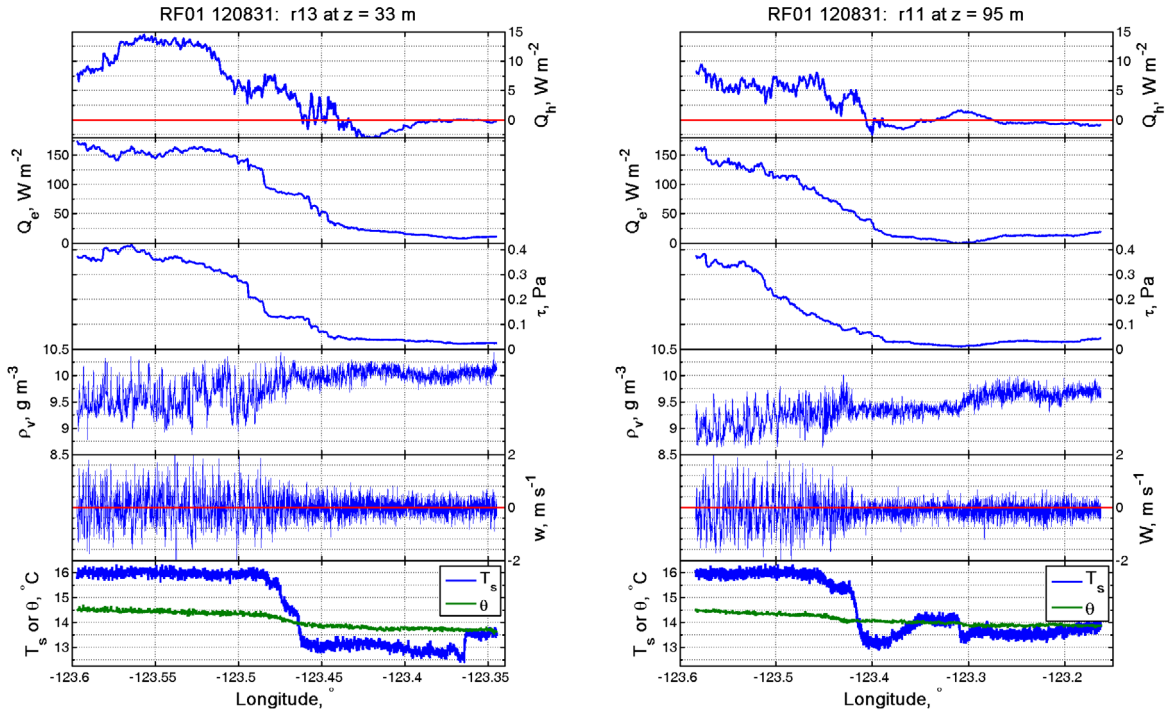

Figure 7. Variations of (from top to bottom) latent heat flux, sensible heat flux, total stress, vertical component of wind, water vapor density, radiometric sea surface temperature and air potential temperature on reciprocal 33-m (left) and ~95-m (right) Twin Otter runs across a strong (~3 ºC) SST front on August 31, 2012. A running averaging technique with a sliding window of 180 s (~10 km) was used for the eddy correlation flux estimates.

A recent addition to the Twin Otter is the "Controlled Towed Vehicle (CTV)" which is a modified target drone that we instrumented for the same turbulence measurements as on the Twin Otter itself. It has been demonstrated to maintain radar altitude height of 10 m above ocean waves while towed from the Twin Otter safely flying 305 m above it as shown in the concept schematic of Fig. 8. The main advantage of the CTV is the direct measurement of stress and associated fluxes at the canonical air-sea interaction height of 10 m.

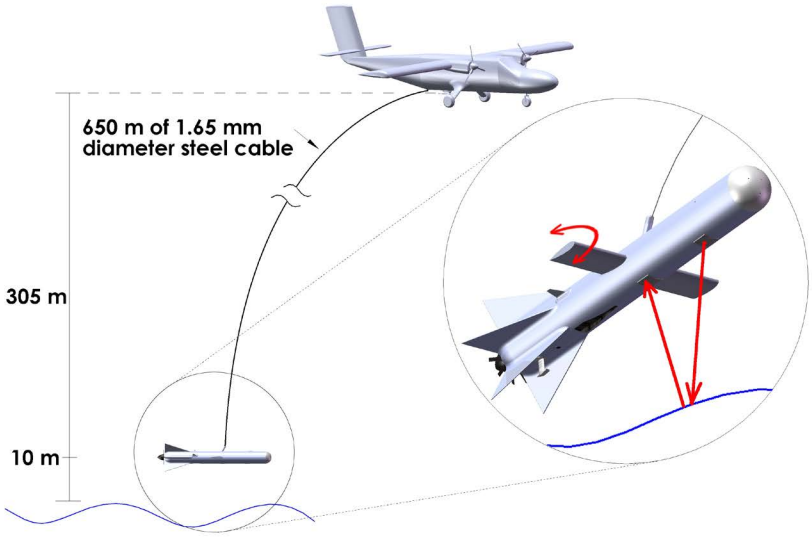

Figure 8. Concept of the Controlled Towed Vehicle (CTV)

Prior to UPPEF, extensive analyses of CTV flights showed that the vertical wind speed contamination by the CTV pitching oscillation was due to the original Meggitt control system being inadequate for the requirements of our application (April 2007 and April 2008) and to leaky pneumatics in the nose gust radome system in addition to a defective angle of attack pressure transducer (UPPEF test flight of July 27, 2012). These problems were corrected before UPPEF. During UPPEF, the CTV was grounded for many days to trouble-shoot problems caused by some undesired modifications that were made to the original (we had back in 2007 and 2008) data system and noisy nose video RF link that allows the flight crew and the CTV operator to detect small vessels that might be ahead of the CTV. In order to operate the CTV at 10 m or so, it is required to have a good enough quality video from the CTV nose camera displayed real-time at the flight deck and at the CTV control station. While the data system was operational by September 18, 2012, the video communication remained problematic throughout UPPEF and the CTV could not be operated below 17 m. The CTV was flown on 6 UPPEF flights (refer to Table 1) and on few shorter flights during the same period that were dedicated to CTV testing. During the 4 last flights, it performed very well albeit it could not be operated at 10 m. Data from the CTV were all processed and the analysis so far has focused on assessing the performance of new CTV control system.

Most of the UPPEF flights were in low to moderate winds conditions with very little wave breaking and hence very little spray to be an issue for AGL laser altimeter used in the control system. There were short lived problems due to very low clouds but in general, performance of the AGL was good.

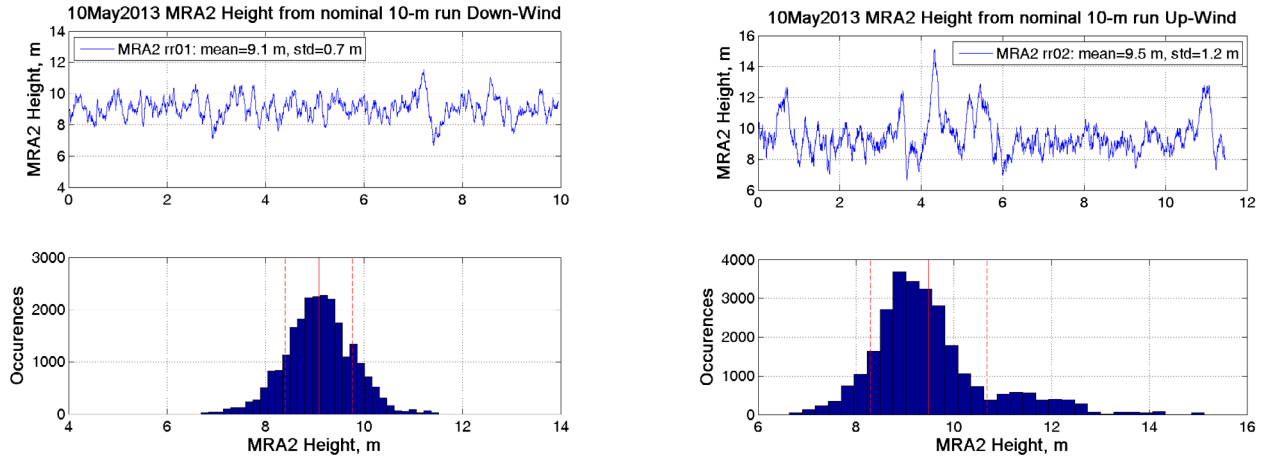

Fig. 9. CTV elevation (top) and histogram (bottom) from MRA2 radar altimeter at a nominal 10-m controlled down-wind (left) and up-wind (right) runs. Altitude mean and standard deviation are given in the insert (top) and shown as solid (mean) and dashed (±σ) red lines (bottom). The CTV height-keeping performed remarkably well at just over 9 m with only 0.7 m standard deviation down-wind and at 9.5 m with 1.2 m standard deviation up-wind.

In order to have a more reliable all weather control system, we decided to replace the laser AGL sensor by the highly accurate Roke Miniature Radar Altimeter Type 2 (MRA2) owned by UCI after making sure the MRA2 performed very well during extensive testing on the Twin Otter during UPPEF. After UPPEF, a great deal of effort was made to integrate the data stream from the MRA2 into the CTV Piccolo autopilot processor and to extensively ground-test the Piccolo/MRA2 control system. On May 10, 2013, we conducted a test flight of the CTV with this new control configuration. The height-keeping performance down to 10 m was very good even in relatively high winds (~15 m s^{-1}) and significant wave breaking for reciprocal (down-wind/up-wind) runs with a total duration over 21 minutes as shown in Fig. 9. The CTV mean radar height was 9.1 m with only 0.7 m standard deviation in the down-wind leg and 9.5 m with 1.2 m standard deviation in the up-wind leg. Albeit occasional excursions to higher elevations during the up-wind leg, the performance is much better than that of the aircraft at 30 m.

The means and standard deviations of the CTV MRA2 elevation from all 19 straight and level runs ranging from ~9 m to ~92 m are shown in Fig. 10. Compared to the higher altitude runs, the lowest runs (~10 m) have a slightly larger standard deviation but it is still very small (less than 1.4 m) considering the high wind and associated waves conditions. The data clearly show that the Piccolo/MRA2 height-keeping system worked very well over the broad range of altitudes. As further evidence of the CTV flight stability and robustness, similar plots for the CTV pitch and roll angles are shown in Fig. 11 The CTV pitches down 3º more at the lowest runs compared to higher ones. This results from the control wing being at its maximum downward orientation of -12º to overcome the lift from the tow cable and maintain the CTV down low. The pitch angle standard deviation, however, remains small (~0.7º) and is about the same for all runs. This is a crucial and an important improvement compared to the original (2007/2008) Meggitt control system that induced very large amplitude and pitching oscillation that contaminated the wind vertical component signal. The roll angle is very small and essentially remains within ±0.5º.

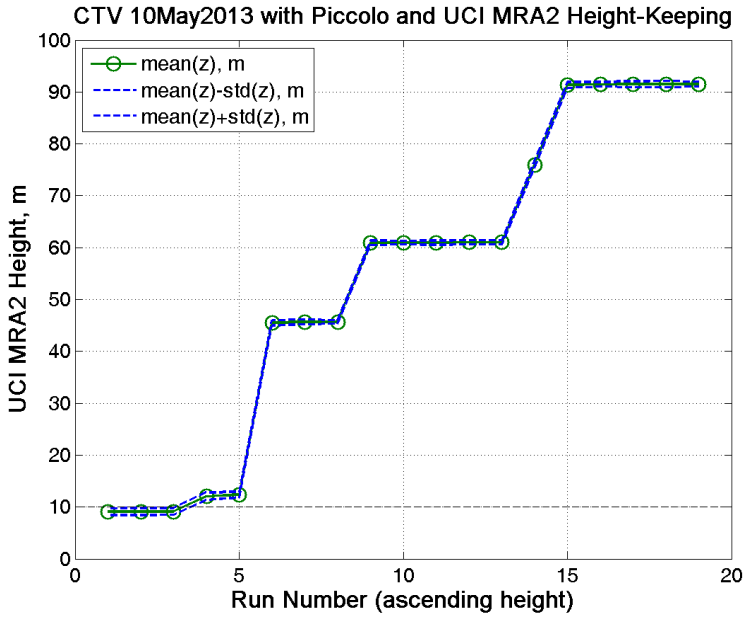

Figure 10: CTV radar altitude from MRA2, z, for all 19 straight and level runs on May 10, 2013: means (green circles and line), ± 1 σ (blue dashed lines). The runs are sorted and numbered from lowest to highest altitudes. Compared to the higher altitude runs, the lowest runs (~10 m) have slightly larger standard deviation but it was still very small (less than 1.4 m) considering the high wind and associated waves conditions. The data clearly show that the Piccolo/MRA2 height-keeping system worked very well even slightly below 10-m.

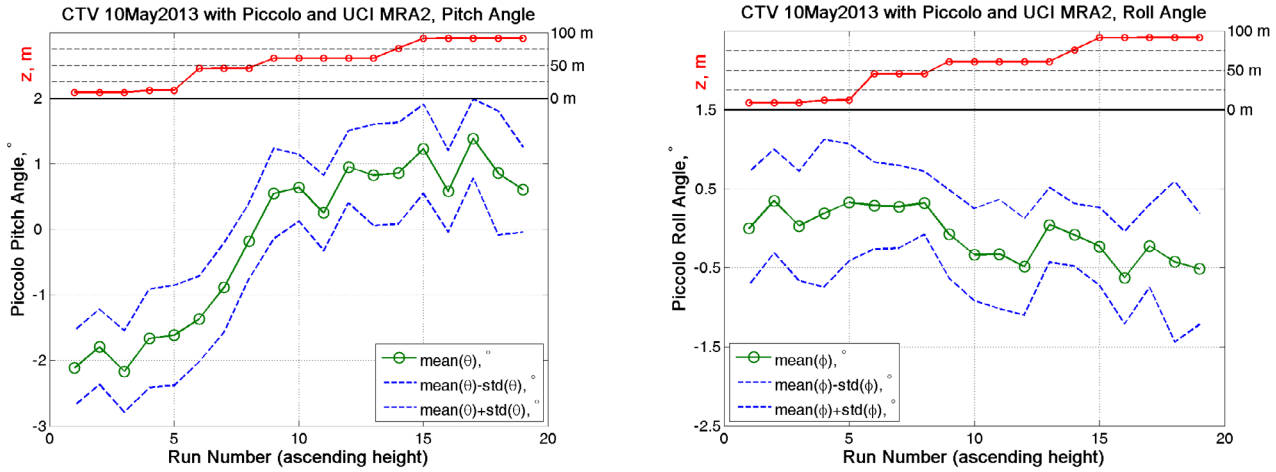

Figure 11: CTV Pitch angle, θ, (left) and roll angle (right) from Piccolo autopilot for all 19 straight and level runs: means (green circles and line), ± 1 σ (blue dashed lines). The runs are sorted and numbered from lowest to highest altitudes. The top red line and circles represent the MRA2 run means with their associated axis on the top left. The CTV pitches down 3º more at the lowest runs but the pitch angle standard deviation remains small (0. 7º) and is about the same for all runs. This is a crucial and a huge improvement compared to the original (2007/2008) Meggitt control system. The roll angle is very small and remains within ±0.5º.

The power spectra densities of vertical component of the wind from CTV runs on 15Apr2007 (original Meggitt control system), 27Jul2012 (AGL laser altimeter and Piccolo autopilot with leaks in radome wind system), 18Sep2012 (AGL laser altimeter and Piccolo autopilot but with "loose" control settings) and finally for 10May2013 (UCI MRA type 2 altimeter and Piccolo autopilot) are shown in Fig. 12. The spectra for 18Sep2012 and 10May2013 no longer exhibit the 0.8-Hz spurious large peak characteristic of the original Meggitt control system (15Apr2007) nor the less energetic 1-Hz peak (27Jul2012) that was attributed to faulty angle of attack transducer and leaks in the radome pressure lines. The wind vertical component is no longer affected by the CTV pitching oscillation whose standard deviation did not exceed 0.62 º during the ~10-m runs.

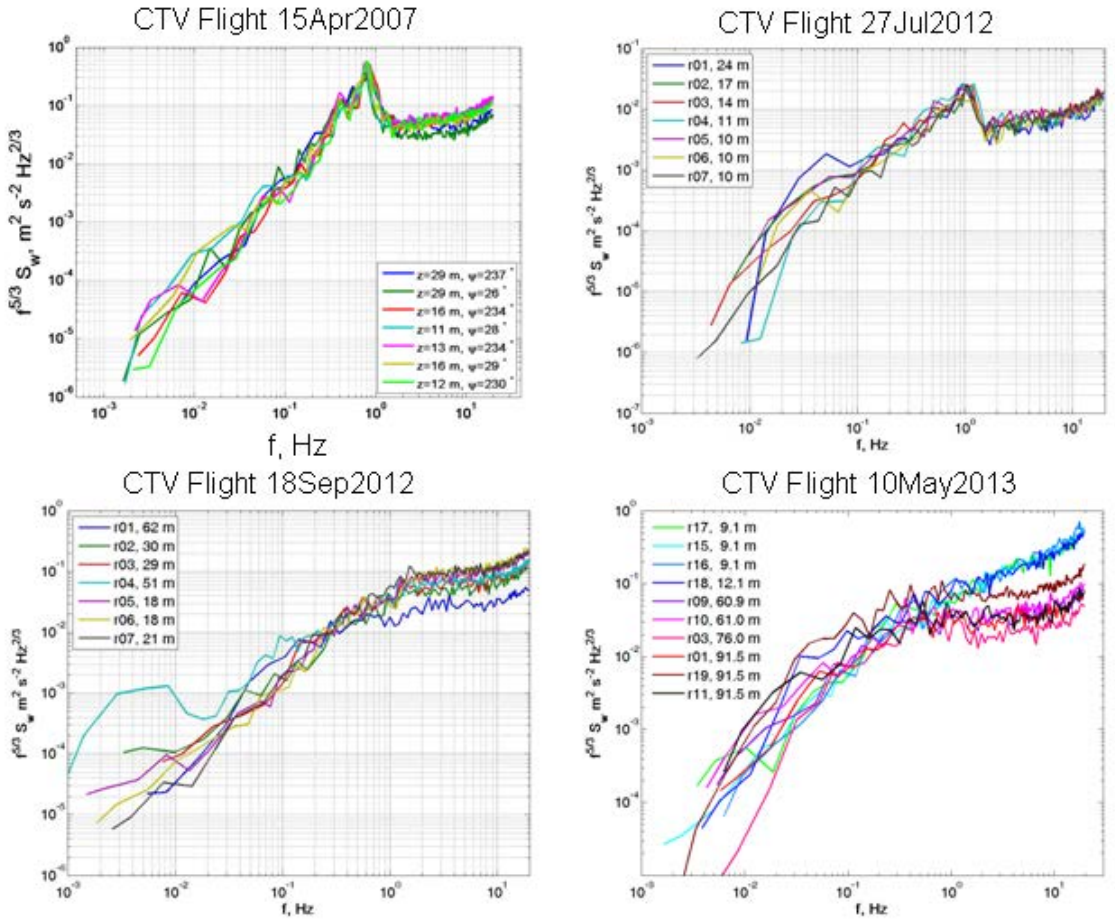

Figure 12: Power spectral densities times frequency$^{5/3}$ of the wind vertical component obtained from CTV flights on 15Apr2007 (top,left), 27Jul2012 (top, right), 18Sep2012 (bottom, left), and on 10May2013(bottom, right). The spectra for 18Sep2012 and 10May2013 no longer exhibit the 0.8-Hz spurious large peak characteristic of the original Meggitt control system (15Apr2007) nor the less energetic 1-Hz peak (27Jul2012) that was attributed to faulty angle of attack transducer and leaks in the radome pressure lines. The -5/3 inertial subrange is resolved up to ~10 Hz for 18Sep2012 and 10May2013 except for the lowest runs on 10May2013 that seem to follow a -4/3 slope . It should be noted that due up-wind and down-wind tracks were flown on 10May2013 instead of the usual cross-wind

One thing of note that was observed and was common to the lowest level runs (z < 14.5 m) on the flight of 10May2013, is that after 2-Hz or so, the vertical wind speed spectra follow a -4/3 slope rather than the -5/3 slope characteristic of the inertial subrange in isentropic turbulence. A possible explanation could be technical: the motion data from the Piccolo used as an alternate are not as good as those of the C-MIGITS which were not usable (due to the start without GPS signal). This does not explain though why it is observed only on the lowest runs. It could also be physical as turbulence statistics are modified by ocean surface waves-induced motion this close to the surface. This was corroborated by recent results by Peter Sullivan from NCAR (shown at the ONR peer-review meeting) he obtained from very high resolution LES model in very similar wind and sampling conditions. Also these flux runs included some slight turns to remain within the cloud-free area as much as possible and to stay at as safe distant from the curvy coast line. These runs were flown roughly on an upwind and downwind track (due to the narrowness of the clear area) instead of the usual crosswind tracks which is most effective for correctly sampling the roll vortices which are roughly aligned with wind direction. The presence of such rolls was also one of the features shown by Peter Sullivan. Furthermore, our own results obtained from analysis of the UCI Met Mast measurements on the stable R/V FLIP during HiRes showed atypical stress divergence in similar conditions in the lowest ~15 meters when the waves phase speed was greater or of the order of the wind speed .

This question of the slope of the vertical wind speed spectra in itself is worth being investigated further, as to our knowledge, this is the first time turbulence data are obtained at ~10 m with an essentially non-intrusive platform (the CTV) compared to ships and buoys whose measurements are notoriously prone to flow distortions and to motion contamination.

IMPACT/APPLICATIONS

The use of the LI-COR 7200 with our modified Rosemount total temperature probe housing used as inlet was successful. It provided reliable and fast response humidity measurements. Our modified krypton hygrometer is a good alternative to the obsolete AIR Lyman-alpha for fast-response humidity measurements from research aircraft.

The CTV height-keeping performance with the new control system we implemented is extremely good even at ~ 9 m above the surface in moderate to strong winds with significant waves breaking and sea spray. The CTV turbulence measurements and in particular the vertical component is of very good quality.

TRANSITIONS

With the major improvements we made to the CTV control and instruments, this platform is ready for use in air-sea interaction research projects.

RELATED PROJECTS

None

PUBLICATIONS

Gerber H., G. Frick, S. Malinowski, H. Jonsson, D. Khelif and S. Krueger, 2013: Entrainment in Unbroken Stratocumulus. [Accepted for publication in J. Geophys. Res.].

Malinowski, S. P., H. Gerber, I. Jen-LaPlante, M. K. Kopec, W. Kumala, K. Nurowska, P. Y. Chuang, K. E. Haman, D. D. Khelif, S. K. Krueger, and H. H. Jonsson, 2013: Physics of Stratocumulus Top (POST): turbulent mixing across capping inversion. [Accepted for publication in Atmos. Chem. Phys.].

Kumala, W., Haman, K. E., Kopec, M. K., Khelif, D., and Malinowski, S. P.: Modified ultrafast thermometer UFT-M and temperature measurements during Physics of Stratocumulus Top (POST), Atmos. Meas. Tech., 6, 2043-2054, doi:10.5194/amt-6-2043-2013, 2013.

Petters, J. L., Jiang, H., Feingold, G., Rossiter, D. L., Khelif, D., Sloan, L. C., and Chuang, P. Y.: A comparative study of the response of modeled non-drizzling stratocumulus to meteorological and aerosol perturbations, Atmos. Chem. Phys., 13, 2507-2529, doi:10.5194/acp-13-2507-2013, 2013.

Mahrt, L., D. Vickers, E. Andreas, and D. Khelif, 2012: Sensible Heat Flux in Near-neutral Conditions over the Sea. J. Phys. Oceanogr. , 42, 1134.1142. doi:10.1175/JPO-D-11-0186.1

Carman, J.K., D.L. Rossiter, D. Khelif, H.H. Jonsson, I.C. Faloona and P.Y. Chuang, 2012: Observational constraints on entrainment and the entrainment interface layer in stratocumulus, Atmos. Chem. Phys., 12, 11135}11152.

Mahrt, L., and D. Khelif, 2010: Heat fluxes over weak SST heterogeneity, J. Geophys. Res. 115, D11103, doi:10.1029/2009JD013161.

Khelif, D., C. A. Friehe, H. Jonsson, Q. Wang, and J. Kalogiros, 2005: Wintertime Boundary-Layer Structure and Air-Sea Interaction over the Japan/East Sea. Deep Sea Research, 52, 1525-1546.